CONF-900291--1

CYCLIC DEFORMATION OF 60Sn-40Pb SOLDER JOINTS DURING THERMOMECHANICAL FATIGUE*

BY

SAND--89-0720C

DE90 004197

Darrel R. Frear
Sandia National Laboratories
Albuquerque, NM 87185

Wendell B. Jones
Sandia National Laboratories
Albuquerque, NM 87185

ABSTRACT

Thermomechanical fatigue and isothermal fatigue tests were performed on 60Sn-40Pb solder joints under a variety of strain ranges and rates. In isothermal fatigue deformation throughout the entire cycle occurs with the same mechanism. The mechanism at low temperatures is a dislocation processes and at high temperatures it is a diffusional flow. In thermomechanical fatigue the deformation mechanism changes in each cycle from dislocation processes to diffusional flow which results in higher peak stresses at the high and low temperature portion of the cycle. This indicates thermomechanical fatigue behavior can not be accurately predicted using isothermal fatigue. It was also found that a decrease in strain rate slowed the heterogeneous coarsening process in thermomechanical fatigue. This is due to the fact that the dislocation substructure recovers more quickly than it work hardens which tends to minimize recrystallization and growth in the solder microstructure.

INTRODUCTION

The introduction of Surface Mount Technology (SMT) has altered the issues in reliability from just a pure electrical standpoint to additional concern over mechanical integrity. Previously, with Plated-Through-Hole (PTH) technology, the electronic packages were constrained to printed wiring boards with pins which offered a robust mechanical design. However, the application of PTH technology is limited by the relatively large physical size of the package and by difficulties in automated assembly. The advantages of SMT over conventional PTH technology are:
i) a reduction in size in both components and boards (and therefore faster switching speeds),
ii) easier automated assembly procedures,
iii) lower overall cost, and
iv) better electrical performance[1].
The main reliability concern in SMT is the mechanical integrity of the solder joints. The failure of a single joint could render a device, or an entire machine, inoperable.

SMT joint failures primarily arise from the imposition of mechanical strain on the joints while in service. This strain is produced when thermal fluctuations act upon the materials of differing thermal expansivities in the package. Thermal fluctuations arise from environmental temperature changes and/or internal Joule heating of the devices. The imposed strain on an SMT solder joint is mainly shear[2], and strains as high as 20% can be induced. The low yield stress of solder allows, for the most part, for the strain to be accommodated through solder plasticity, but upon repeated cycling the solder joints can fail in fatigue[3-6]. Therefore it is essential to develop a fundamental understanding of the metallurgical processes that lead to the thermomechanical fatigue failure of solder joints. Once the thermomechanical fatigue process is understood, methods to alleviate or eliminate these failures can be determined.

One fundamental aspect of thermomechanical fatigue of solder is the relationship between the mechanical response (stress development) and microstructural evolution to cyclical temperature and strain cycles. This paper explores this relationship as a function of imposed strain and strain rate in thermomechanical fatigue. Included in this study is the effect of temperature in isothermal fatigue. The goal of this work is to determine the stress behavior of solder joints and relate this to standard classical low cycle/creep deformation mechanics.

* This work performed at Sandia National Laboratories, Albuquerque, New Mexico, 87187-5800 and supported by the U.S. Department of Energy under contract number DE-AC04-76DP00789

CYCLIC DEFORMATION OF 60SN-40PB SOLDER JOINTS DURING THERMOMECHANICAL FATIGUE
By D. R. Frear and W. B. Jones

EXPERIMENTAL PROCEDURE

A summary of the procedure used to test solder joints in thermomechanical fatigue is given below. A more detailed description of the testing apparatus is given elsewhere[7].

The specimen used for these tests is shown in Figure 1; it is a modification of a double shear specimen[8]. The sample is comprised of three plates (Figure 1A). The plates are a fiberglass impregnated epoxy upon which Cu lines and lands have been imprinted, and all but the lands are covered with solder resist. The lines are used for electrical detection of failures and are not wet by the solder. The center plate has a mirror image on the front and back. Each outside plate has Cu lands on both sides with a plated-through-hole connecting the inside to the outside. When the sample is soldered together electrical continuity exists through each individual solder joint from the center plate to the outside plate. The Cu lands were fluxed, "pre-tinned" with 60Sn-40Pb solder, and then cleaned with acetone to remove any remaining flux residue. When the sample is assembled, as shown in Figure 1B, side spacers are inserted between the plates to provide a gap for the joints to form. The sample is then dipped, lengthwise, into a molten solder bath for one minute, removed and allowed to cool. The solder only wets at the pre-tinned lands so that 18 electrically isolated solder joints make up each specimen.

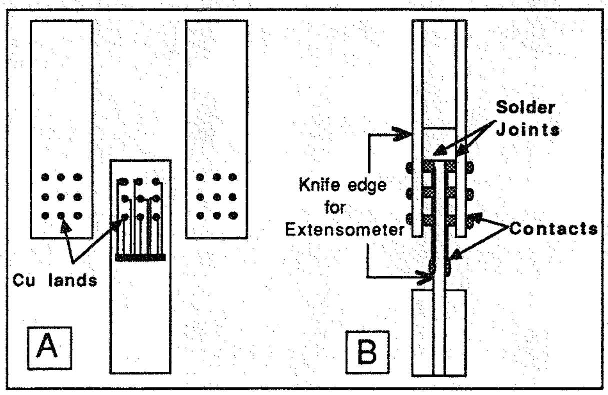

Figure 1 Schematic illustration of double shear specimen. A) Before and B) After assembly.

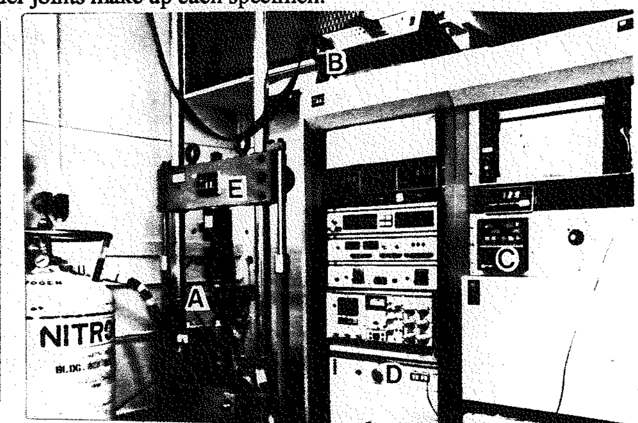

Figure 2 Photograph of thermomechanical test apparatus. A: Thermal chamber, B: Event Detector, C: Temperature Controller, D: Loadframe control, E: Loadframe.

Deformation was imposed on the specimen by a computer controlled servo-hydraulic system operated under strain control. Displacement was measured with a knife edged extensometer accurate to ±0.5% and was attached to the specimen as shown in Figure 1. The knife edges were not observed to show any slippage during testing. The shear strain was calculated from:

$$\gamma_o = \delta/t \qquad (1)$$

where γ is the calculated shear strain, δ is the imposed axial displacement, and t is the solder joint thickness. The load was measured using a 10 kip load cell accurate to ±0.25%. The DEC LSI 11/34 computer also collects digital data obtained during the test and stores it on hard disk.

The heating and cooling was accomplished using a thermal chamber that fits around the specimen. A fan circulated air through the chamber and past the specimen. Hot air for the heating portion of the cycle was created using resistive coils in the chamber. The cooling portion of the cycle was produced by bleeding liquid nitrogen into the chamber which vaporizes and thereby cools the recirculating air. The temperature cycling itself was controlled by a digital temperature controller which was in turn controlled by the loadframe computer.

To determine failures a continuity monitoring technique was developed. An event detector continuously monitored 16 individual solder joints. Failures were determined by the presence of a persistently detected spike in resistance over 5000Ω, which is indicative of a crack that has propagated through the solder joint. A joint was determined to have failed when 15 of these spikes had occurred. A spike event is defined as an intermittent or transient resistance fluctuation that exceeds 5000Ω and has a duration of at least 0.2 μs. Figure 2 is a photograph of the assembled thermomechanical fatigue test apparatus.

CYCLIC DEFORMATION OF 60SN-40PB SOLDER JOINTS DURING THERMOMECHANICAL FATIGUE
By D. R. Frear and W. B. Jones

Two types of fatigue tests were performed on the 60Sn-40Pb solder joints. Isothermal (constant temperature) tests were performed at 10% total strain and three temperatures: -55°, 23°, and 125°C. The calculated shear strain rate in isothermal fatigue was 5.5×10^{-4} /s. Thermomechanical fatigue tests were performed over the temperature range of -55° to 125°C for the strains and rates listed in Table 1. Both the isothermal and thermomechanical fatigue tests used the same trapezoidal thermal/strain waveform. For all but the slower 20% strain test, this consisted of a 3 minute ramp up and 3 minute ramp down with 3 minute hold times at each extreme. The 20% slow strain rate test increased the ramp time to 12 minutes with the hold time remaining at 3 minutes.

Table 1. Summary of test conditions.

Strain range (%)	Cycle time (min)	Displacement rate (μin/s)	Shear strain rate (/s)
5	12	2.8	2.8×10^{-4}
10	12	5.5	5.5×10^{-4}
20	12	11.0	1.1×10^{-3}
20	30	2.8	2.8×10^{-4}

A note should be made regarding the hysteresis behavior for the fatigue tests presented in this work. Each hysteresis loop represents the collective response of the 18 solder joints of each specimen. Accordingly, the translation of the load *vs.* displacement loops measured during testing into material stress *vs.* strain behavior must be done with great caution. Two factors mitigate to make this an uncertain process. First, crack formation and growth in individual joints will result in a load decrement so that any decrease in load that was observed could not be unambiguously assigned to either joint cracking or cyclic softening of the Pb-Sn alloy. These two independent effects cannot be separated in our tests. Second, the imposed strain range for each test was based on a the simple shear strain calculation given in Equation 1. This assumes that the displacement, δ, is distributed uniformly over the thickness of the solder joint. Earlier work has shown that heterogeneities within the joint develop which tend to localize this displacement into a much narrower band of solder [9-11]. The local shear strain is then nowhere the average (γ_o) calculated by Equation. 1; but is, instead, less than γ_o across most of the joint, and greater than γ_o across the heterogeneous band through which the fatigue crack eventually grows. The loops shown in this paper are taken at cycle N=5 in order to show sample response for which these complicating factors are minimal.

RESULTS

1. Isothermal Cycling

Figure 3 shows a schematic hysteresis loop for the strain cycle developed by this test with several key points indicated in subsequent figures. Also included in Figures 4-6 are optical micrographs of the microstructure of the solder joint for each temperature.

At -55°C there is very little hysteresis in the load-displacement response and no noticeable relaxation during the 3 min. dwell time at each peak, as shown in the hysteresis loop in Figure 4A. The slope of this curve is 4.8×10^4 psi while the unrelaxed elastic shear modulus is 8.4×10^5 psi at this temperature[12]. Figure 4B shows that the peak stresses remain essentially unchanged and that there continues to be no observable relaxation during the dwell periods for testing up to 200 cycles. Figure 4C shows the microstructure of the -55°C test after 200 cycles. No cracks were observed in any of the joints. Furthermore the microstructure is still very fine, no coarsening of any kind was observed, and is similar to the as-soldered condition. These observations would indicate that the behavior shown in Figure 4B reflects a stability in the mechanical response of the solder during stress cycling, with neither hardening nor softening taking place.

Figure 5A shows that at room temperature (23°C) significant relaxation is observed. The hardening slope begins at about 4.8×10^4 psi on loading from ~~the dwell~~ period and decreases to 2.6×10^4 psi at the opposite strain limit. The shear modulus at room temperature for eutectic Pb-Sn is 7.7×10^5 psi. At 23°C, the relaxation shown in Figure 5B is seen to persist throughout the test and it occurs at about the same fraction of peak stress. Figure 5C shows the microstructure after 100 cycles at 23°C. The microstructure of this sample shows heterogeneous coarsening parallel to the direction of imposed shear and also coarsening at cell boundaries. Cracks were observed in the joints through the heterogeneous coarsened regions. It is interesting to note that the structure within the cells is still fine, all coarsening is concentrated at the cell boundaries. The load decrease shown in Figure 5B is due, in part, to the development of this cracking.

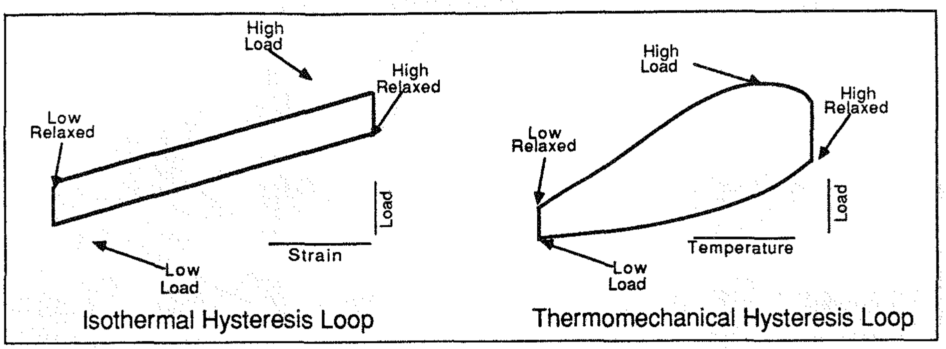

Figure 3 Schematic illustration of a load - strain hysteresis loop showing points used in subsequent figures.

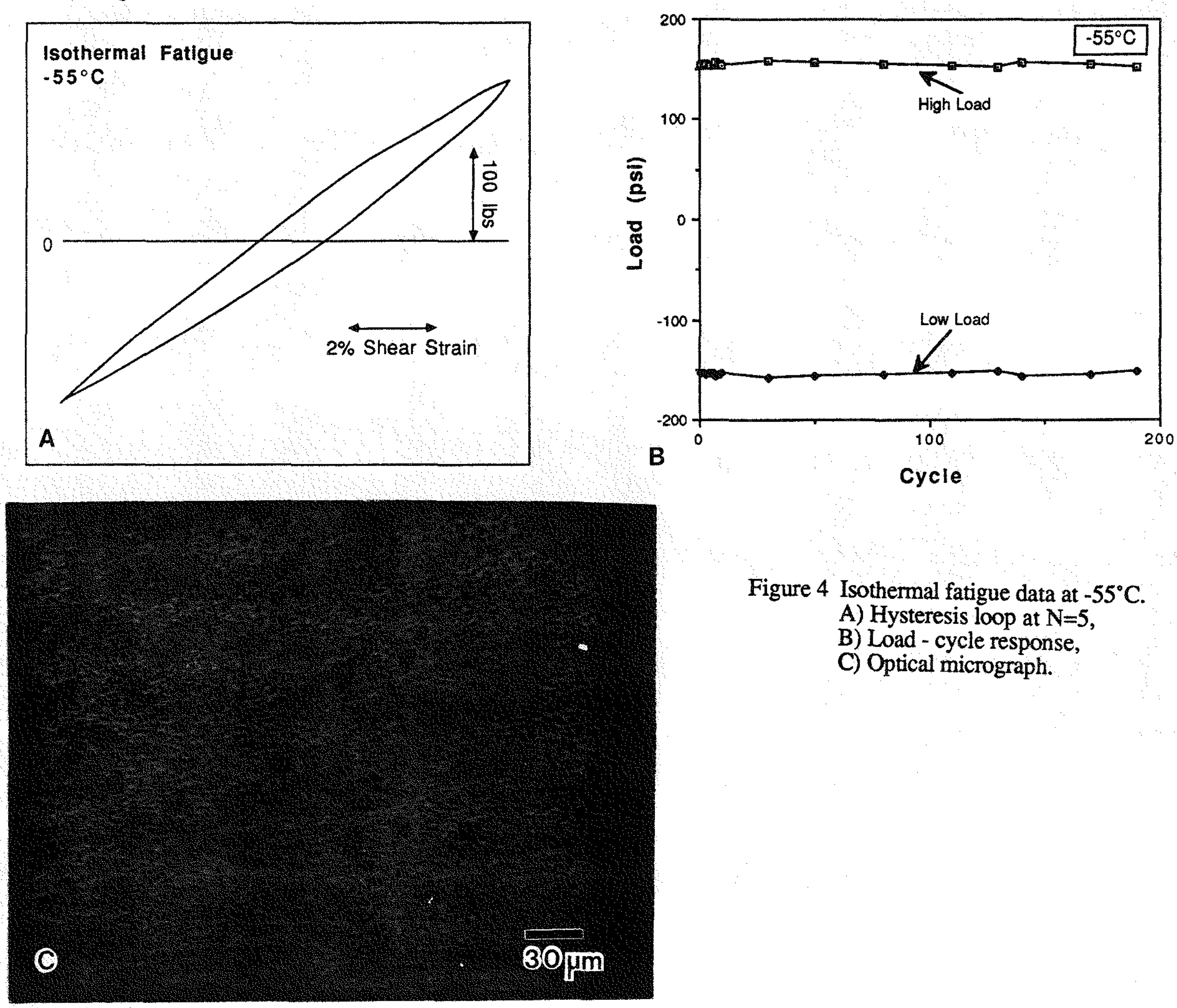

Figure 4 Isothermal fatigue data at -55°C.
A) Hysteresis loop at N=5,
B) Load - cycle response,
C) Optical micrograph.

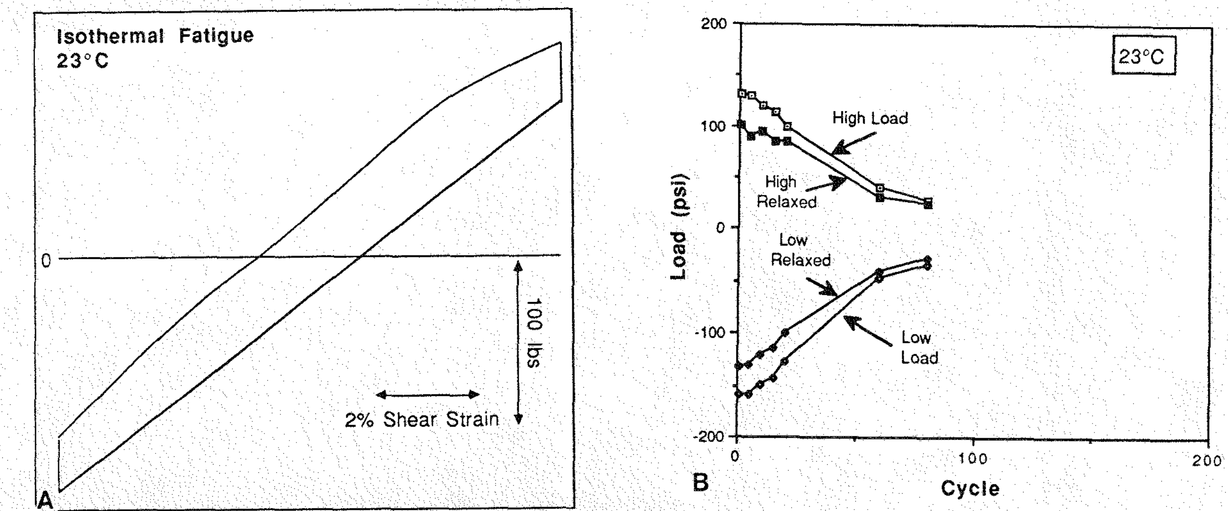

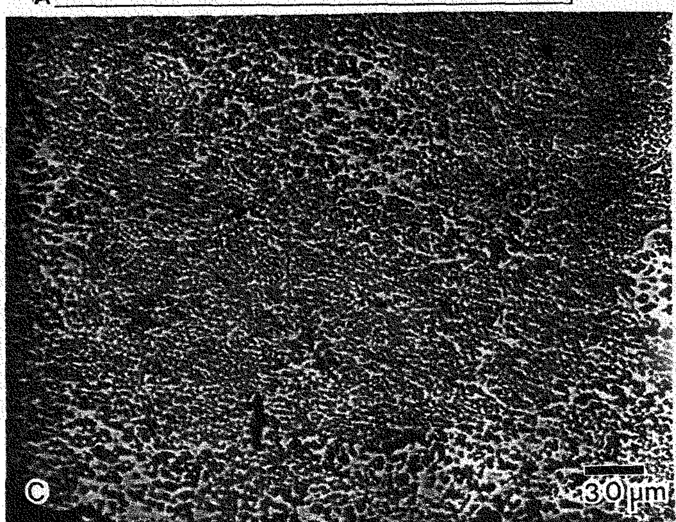

Figure 5 Isothermal fatigue data at 23°C.
A) Hysteresis loop at N=5,
B) Load - cycle response,
C) Optical micrograph.

Figure 6A shows the hysteresis behavior resulting from cycling at 125°C. The stress levels developed at this temperature are greatly diminished relative to the lower temperature tests. The work hardening at this temperature decreases to 9.4×10^2 psi at the strain limit after beginning at 1.8×10^4 psi at the start of reloading. The shear modulus at this temperature is 3.6×10^5 psi. This is a similar type of behavior as was found for the room temperature tests and these results are summarized in Figure 6B. The stress magnitudes are much lower, but the degree of relaxation over the duration of the test remains relatively unchanged. Figure 6C shows the solder microstructure after 100 cycles at 125°C. Coarsening is extensive throughout the joint. Heterogeneous coarsened bands were observed as well as coarsening at the cell boundaries and within the cells themselves. Extensive cracks were observed in the joints through the heterogeneous coarsened regions, which is reflected in the decreasing load response shown in Figure 6B.

2. Thermomechanical Cycling

The load-displacement response under conditions of thermomechanical cycling is much more complex. Figures 7 and 8 show the specimen response under four different conditions. These are given as temperature *vs.* load. Any interpretation of the load in terms of stress must be done with caution, as discussed above. The free expansion and contraction of the specimen

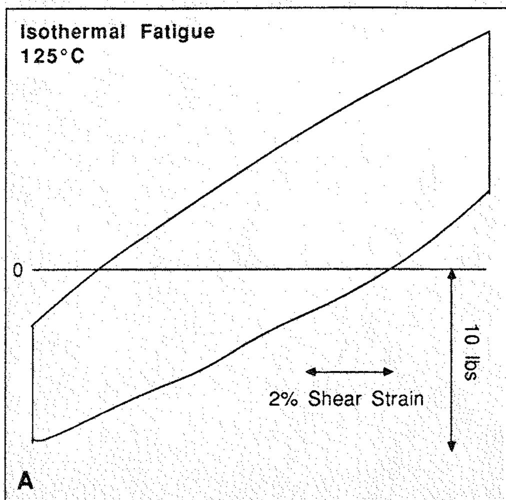

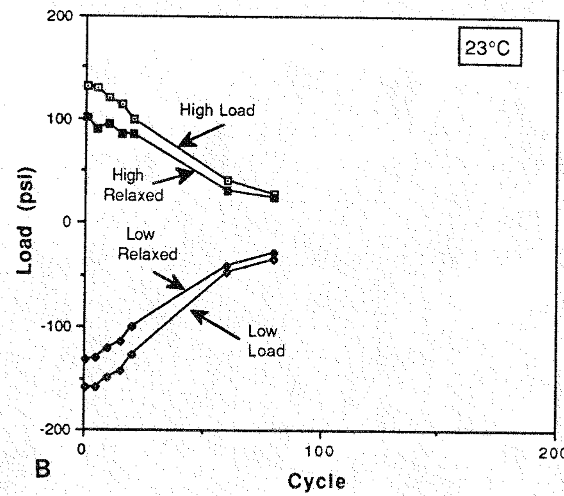

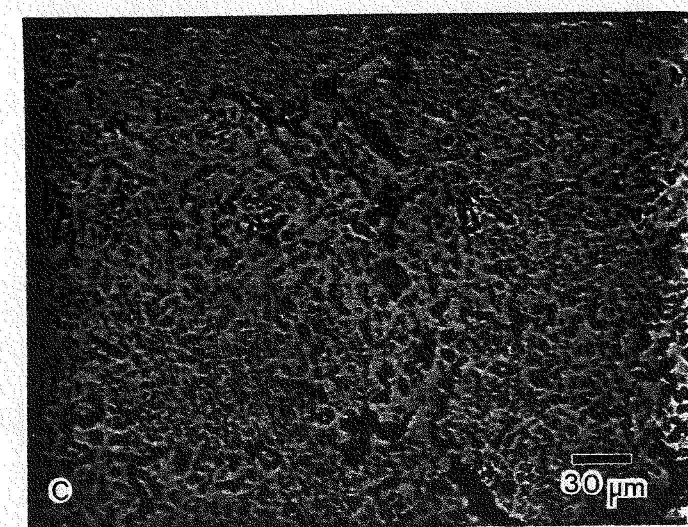

Figure 6 Isothermal fatigue data at 125°C.
A) Hysteresis loop at N=5,
B) Load - cycle response,
C) Optical micrograph.

across the temperature range -55 to 125°C is about 2.0%. The tests at 5%, 10%, and 20% strain range therefore represent differing degrees to which this natural change must be augmented to produce the desired strain ranges.

The responses shown in Figures 7 and 8 reflect the strong dependence of flow stress for this alloy across the temperature range of the tests. All show some degree of work softening as the cycle nears the peak temperature. Also present is enhanced work hardening as the temperature is decreased toward the minimum. Figure 8 shows the marked effect of changing the cycle period from 12 min/cycle to 30 min/cycle. The magnitude of the stresses during the increasing temperature portion of the cycle are decreased to near zero at the longer cycle time. There is also virtually no work softening as the peak temperature is approached when the cycle time is 30 min compared to the marked softening for the shorter cycle time. The longer cycle time also results in less relaxation during the dwell time at the minimum temperature.

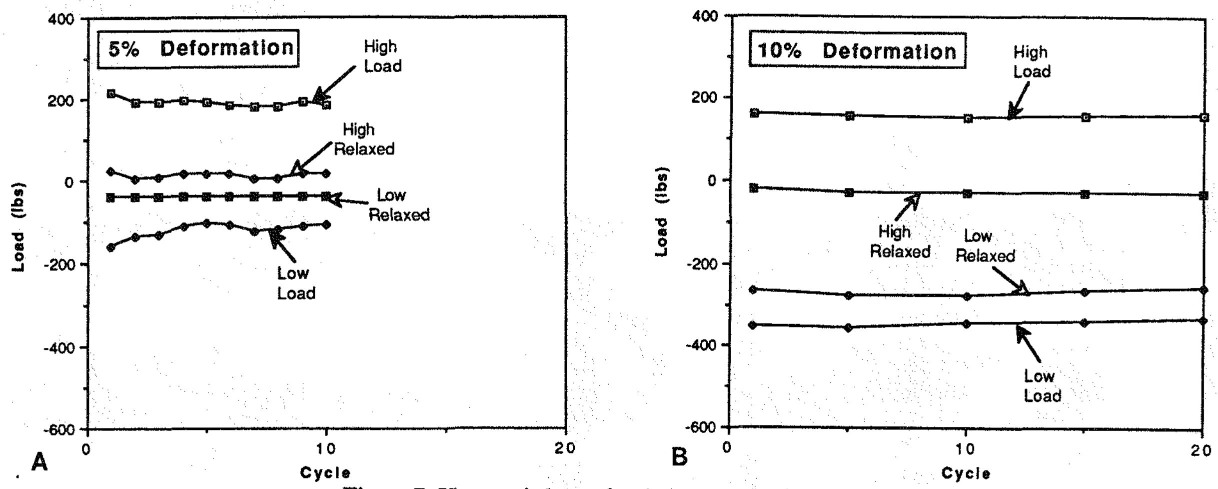

Figure 7 Hysteresis loops for thermomechanical cycling tests
A) 5% strain range
B) 10% strain range

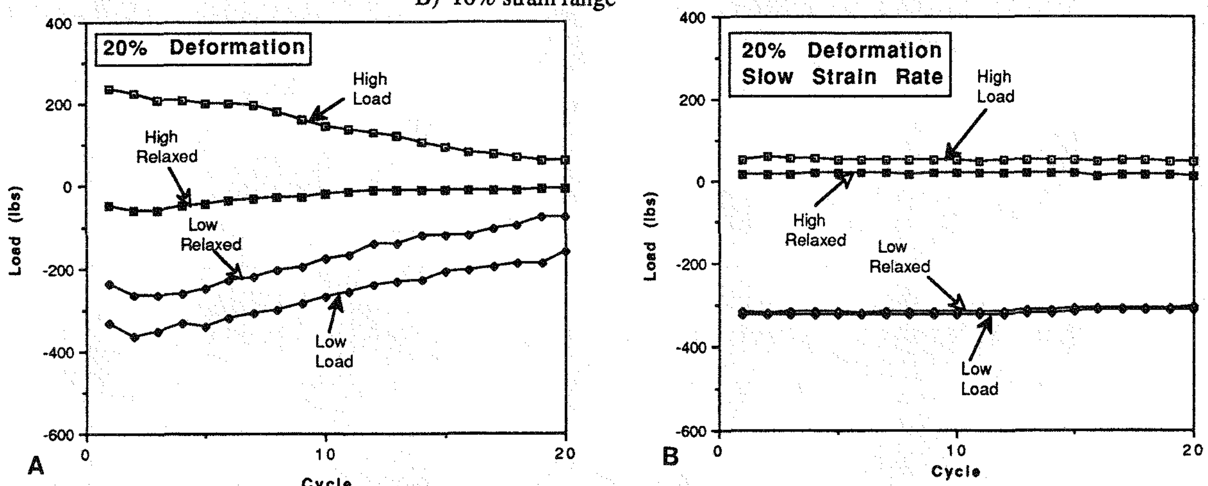

Figure 8 Hysteresis loops for thermomechanical cycling tests at 20% strain range
A) 12 min/cycle
B) 30 min/cycle

Figure 7 shows that the stress levels were approximately constant during the first several cycles. At 5% strain range, the relaxations during the dwell periods were nearly complete, taking the stress to near zero. The stress magnitude at the hot end of the cycle was actually higher than at the cold end for the 5% strain cycle. For 10% strain range, the stress peaks were approximately balanced and the degree of relaxation at the cold temperature was limited compared to the relaxations which occur at the maximum temperature. This is similar behavior to that shown in Figure 8A for 20% strain range cycling at 12 min/cycle. When the cycle time is lengthened to 30 min., a very different response is produced (Figure 8B). The peak stress at the minimum temperature is similar for the two cycle times, but all other features are different. The peak stresses at the maximum temperature are very small, and, accordingly, the extent of relaxation is also minimal. These peak load levels remain constant out to 20 cycles for the longer cycle time compared to the distinct load fall-off noted in Figure 8A for the shorter cycle time.

CYCLIC DEFORMATION OF 60SN-40PB SOLDER JOINTS DURING THERMOMECHANICAL FATIGUE
By D. R. Frear and W. B. Jones

The microstructural response of the solder joints to the variety of strain conditions in thermomechanical fatigue is as complex as the load displacement response discussed above. Figure 9 is an optical micrograph of a solder joint after 20% strain at a strain rate of 1.1×10^{-3} /s for 10 cycles. Extensive heterogeneous coarsening is observed with cracks propagating through the coarsened regions. However, no crack was detected electrically or by metallurgical observation to have completely propagated through any of the 18 joints. Figure 9 is a classic example of the heterogeneous coarsened region providing a path for crack propagation. Figure 10 shows another joint where the heterogeneous coarsened band formed between two cells with very clear boundary definition.

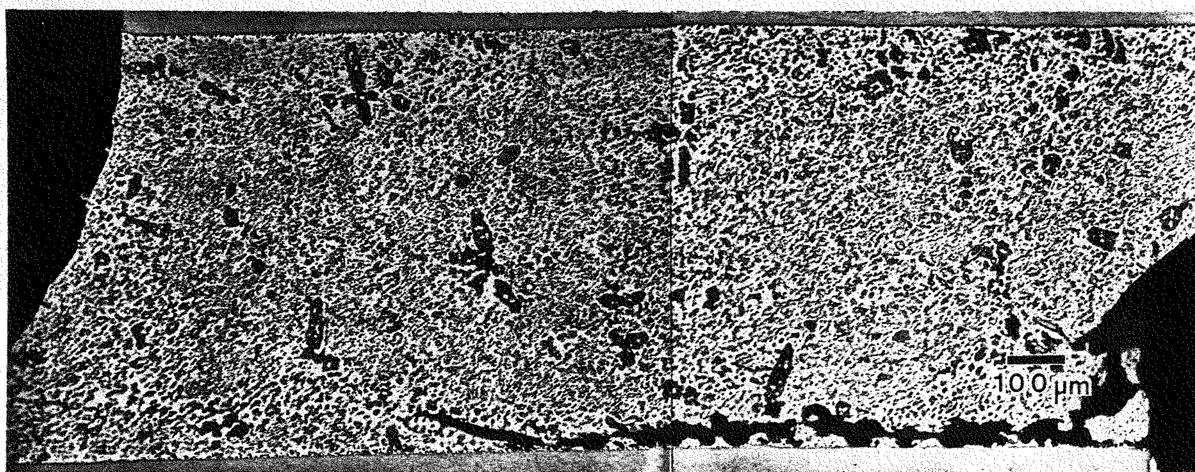

Figure 9 Optical micrograph of solder joint after 10 cycles at 20% strain with a strain rate of 1.1 x 10-3 /s.

Figure 10 Optical micrograph of solder joint after 10 cycles at 20% strain with a strain rate of 1.1 x 10-3 /s showing a clearly defined coarsened region.

Figure 11 shows the microstructure of a solder joint subjected to 10% strain cycling at a strain rate of 5.5×10^{-4} /s for 10 cycles. Again this sample had no electrical failures but heterogeneous coarsening was found with some cracks in the coarsened regions. In this micrograph no cracks were found but a heterogeneous coarsened region in the solder was observed (as is indicated by arrows). The heterogeneous coarsened regions in this sample were not as well defined as those in the sample strained at the 20% strain range.

The sample with 10 cycles at 5% strain range and a rate of 2.8×10^{-4} /s is shown in Figure 12. No cracking was observed in this sample. There does not appear to be any heterogeneous coarsening present although cell boundaries appear to have a coarser morphology. Apparently at this strain range and rate, heterogeneous coarsening does not occur for this small number of cycles.

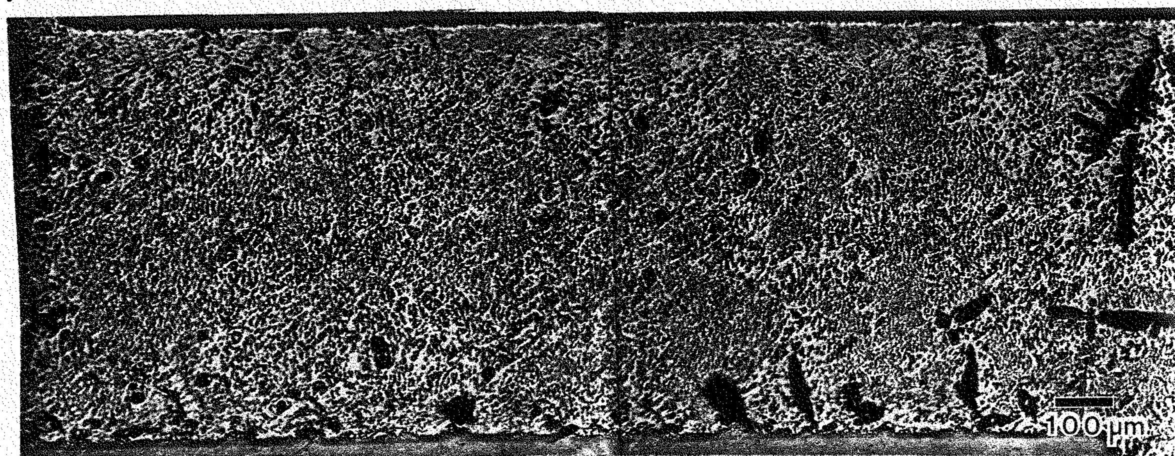

Figure 11 Optical micrograph of solder joint after 10 cycles at 10% strain with a strain rate of 5.5×10^{-4} /s.

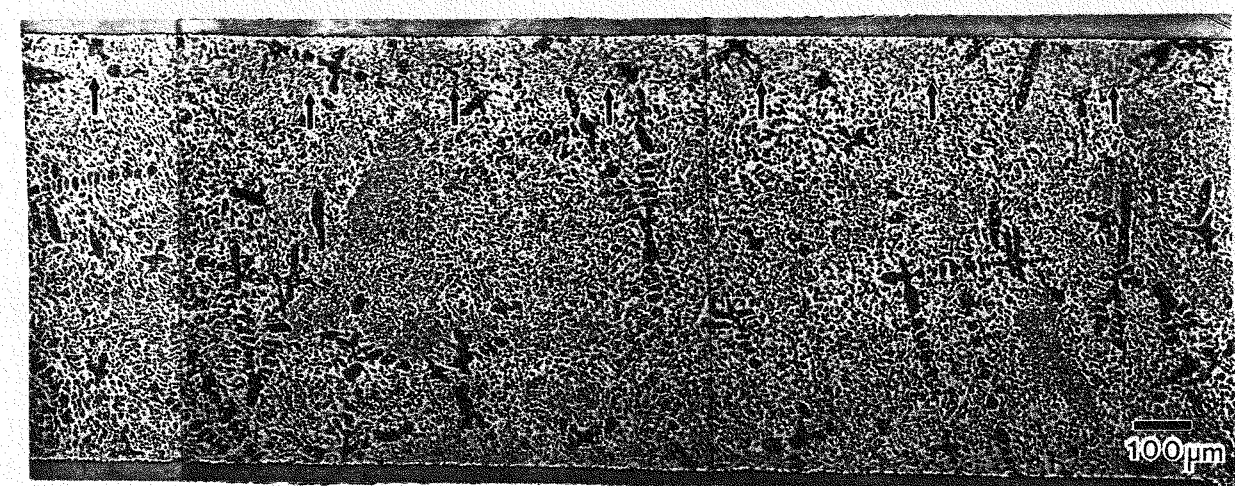

Figure 12 Optical micrograph of solder joint after 10 cycles at 5% strain with a strain rate of 2.8×10^{-4} /s.

The effect of varying the strain rate on the microstructure is shown in Figure 13 for a sample after 20 cycles at 20% strain range at a slow strain rate of 2.8×10^{-4} /s. This was chosen to be the same rate as the 5% strain range sample discussed above. To achieve this strain rate the thermal cycle was increased to 12 minute ramp times with 3 minute holds at each extreme temperature. The microstructure of this sample shows some coarsening at cell boundaries, but no definable heterogeneous coarsening. Furthermore, no cracks were observed in any of the joints tested. The microstructure for the 20% strain, 30 minute cycle more closely resembles that shown in Figure 12 for the 5% strain than that in Figure 9 for the 20% strain at 12 minutes per cycle.

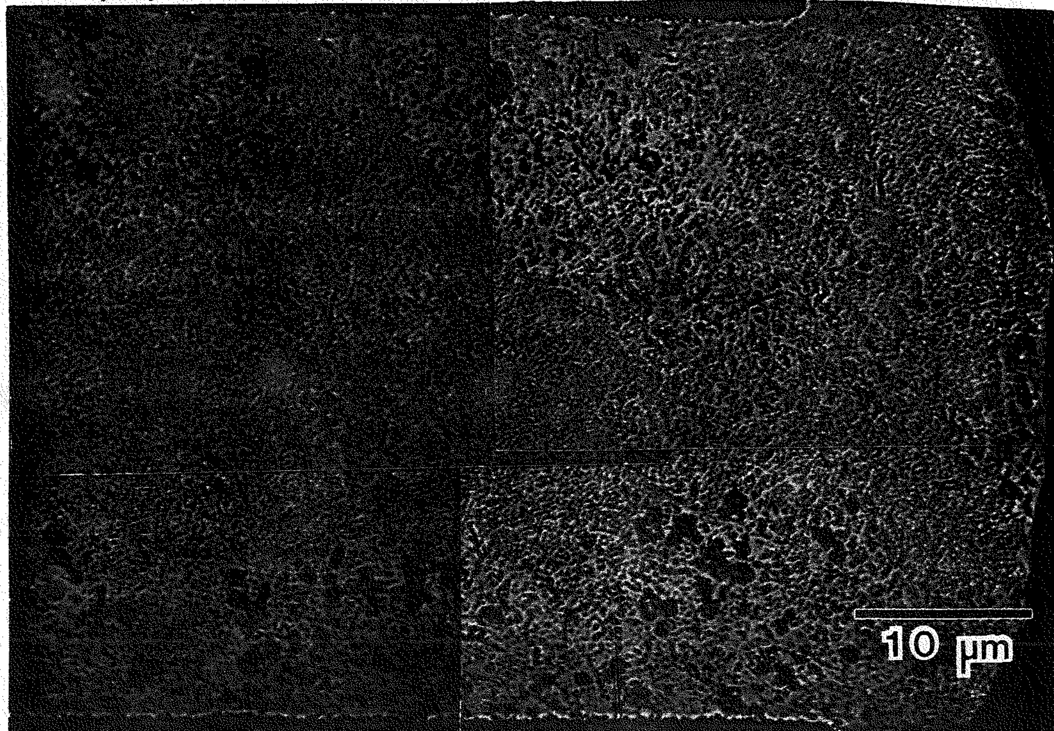

Figure 13 Optical micrograph of solder joint after 20 cycles at 20% strain with a strain rate of 2.8×10^{-4} /s.

DISCUSSION

These data embody a large number of features which invite discussion; however, we will focus on two in the remainder of this paper. First, we will discuss the differences between isothermal and thermomechanical fatigue, and second, we will discuss the effect of strain rate in thermomechanical fatigue.

The isothermal fatigue responses shown in Figures 4-6 are indicative of the behavior of an alloy cycled at very high homologous temperatures ($T_h = T/T_{mp}$). Figure 14 shows the flow stress at the 5% strain limit for the 5.6×10^{-4} /s strain rate for each of the three temperatures used in this study. The lack of any cyclic hardening in the samples cycled at -55° C indicates that even at the lowest temperature, that work hardening and recovery are approximately balanced for each cycle, *i.e.* there is no net buildup or loss of dislocations from cycle to cycle leading to hardening or softening. Also, the photomicrographs show that there is no evolution in the overall microstructure during these tests. At the higher temperatures, the microstructural evolution observed would be expected to lead to local softening of the matrix and the increased role of dislocation recovery processes at these higher temperatures would also be expected to lead to cyclic softening. While the data in Figures 4-6 reflect this, those changes will also be influenced by the development of cracks in the individual joints.

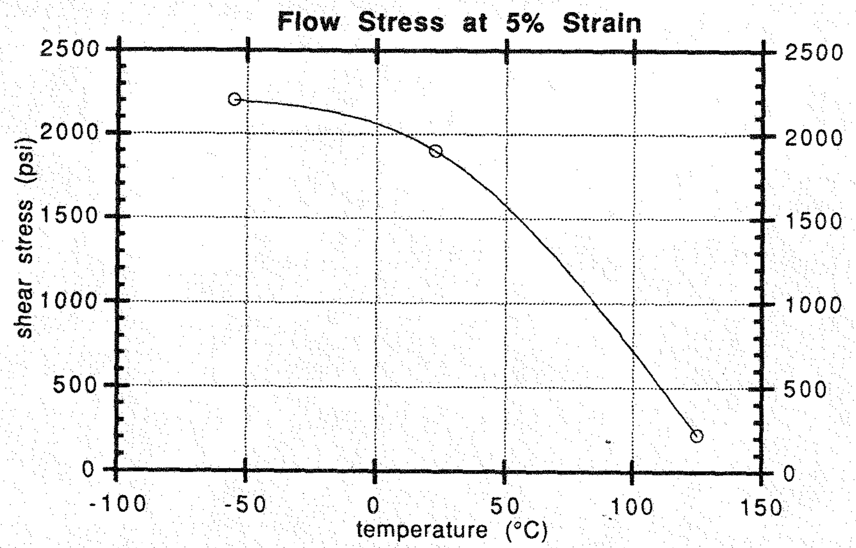

Figure 14 Plot of flow stress as a function of temperature for thermomechanical fatigue at 5% strain.

Due to the fact that these tests are isothermal, the deformation throughout the cycle occurs by the same mechanism and at the same balance of work hardening and recovery. It is interesting to note that there is very little relaxation during the dwell periods for the tests conducted at -55°C. This temperature represents a homologous temperature of 0.48 which is certainly high enough to have extensive time dependent deformation (like creep and relaxation). The lack of any relaxation is an indication of the stability of the dislocation structure that is developed during the cycle at this strain rate and a reflection that dislocation mechanisms dominate the creep and relaxation behavior in this situation[14]. At the higher two temperatures, diffusional flow mechanisms dominate during relaxation and significant relaxation occurs. Under this thermal activation, local coarsening occurs which results in a band of coarser structured, lower flow stress material[11].

Thermomechanical cycling produces a different but predictable response. The key feature in interpreting these differences is the change in deformation mechanism from dislocation processes at -55°C ($T_h = 0.48$) to diffusional flow processes at 125°C ($T_h = 0.87$)[14]. The hysteresis loops in Figures 7 and 8 reflect several features to be discussed. First is the distinctive work softening near the peak maximum temperature. For the 12 minute cycle time, the magnitude of this effect increases with increasing strain range (Figures 7A, 7B, and 8A). During the portion of the cycle at lower temperature, large dislocation densities are developed which leads to larger than expected peak stresses as the temperature is increased. As the temperature rises toward the maximum, recovery process occur at a rate fast enough to overwhelm work hardening and the stress level begins to decrease toward the steady state flow stress at that strain rate. These dislocation recovery processes and the diffusional flow processes continue during the dwell period. The temperature and strain ramp from the maximum to the minimum temperature is characterized by the increase in flow stress that occurs as the temperature is decreased. The dynamic steady-state observed in the isothermal test at -55°C is not present here, and significant relaxation occurs during the dwell at the peak cold temperature. Comparing Figures 4A, 6A, and 7B show that the superposition of isothermal tests will not adequately predict the thermomechanical test results. Table 2 summarizes this comparison. The isothermal test result would severely underestimate the peak stresses developed by the thermomechanical test. In addition, most damage accumulation schemes involve the use of ~~one or~~ several parameters which are related to the hysteresis area[15] and this parameter would also be underestimated by using only the isothermal tests.

Table 2. Comparison between isothermal tests at -55°C and 125°C and a thermomechanical test, all at 10% strain range.

	-55°C, peak (psi)	-55°C, relaxed (psi)	125°C, peak (psi)	125°C,relaxed (psi)
isothermal fatigue	-2200	-2200	220	70
thermomechanical fatigue	-2300	-1650	1400	100

The effect of strain range can be seen by comparing Figures 7A, 7B, and 8A. Qualitatively, these results are very similar. The extent of work softening increases with increasing strain range and the temperature at which the stress reaches a peak decreases with strain range. These effects reflect the development of dislocation structures which reach a higher dislocation density at the higher strain range (*i.e.* higher peak stresses at lower temperatures), and this higher dislocation density leads to significant recovery at slightly lower temperatures. It is important to note again here that the cycle time for the tests discussed here remained constant while the strain range was varied between 5% and 20%. Thus, the strain rate also increased by a factor of four.

Varying the strain rate in thermomechanical cycling had a very large effect on the microstructure of 60Sn-40Pb solder over the rates tested. It appears, in fact, that the testing rate has a stronger influence than does the total strain imposed. The samples tested at 2.8×10^{-4} /s showed very similar microstructures after both 5% and 20% imposed shear strain range, Figures 12 and 13. In these cases slight coarsening of cell boundaries with little or no heterogeneous coarsening and no cracks were observed. Conversely the sample tested at 20% strain range and four times the rate, 1.1×10^{-3} /s, exhibited extensive heterogeneous coarsening with cracks through the heterogeneous coarsened regions and after 10 cycles was on the verge of failure. An even higher strain rate was tested previously[9-11] using thermal shock where solder joints constrained between materials with differing thermal expansivities (Cu and Al) were cycled between 125° and -55°C baths. The total imposed strain in that test was 20% and the displacement rate was approximately 4.0×10^{-3}/s. In these samples the heterogeneous coarsened regions were very well defined and were the only part of the microstructure that coarsened; cracks were found within the coarsened bands. This same observation has also been made on isothermal fatigue tests performed at high strain rates[13].

An explanation for these differing microstructures with varying strain rates can be developed by examining the proposed mechanism by which the heterogeneous coarsened regions form[9]. At the low temperature potion of the cycle, deformation concentrates at the weakest parts of the microstructure which are the slightly coarsened regions at the cell boundaries parallel to the direction of shear. Upon heating and deforming to the high temperature portion of the cycle, these regions coarsen further due to the presence of dislocations which act as sites for recrystallization and growth and are also rapid diffusion paths. Further cyclic deformation continues to concentrate in these regions resulting in further heterogeneous coarsening and eventual failure.

The mechanism described above appears to remain valid for the higher strain rates. However, for low strain rates this heterogeneous coarsening mechanism appears to be delayed. This may be due to the dynamic recovery that occurs during deformation. The extensive dynamic recovery in the thermomechanical tests has already been discussed. At the higher strain rate, Figure 8A, a great deal of work hardening occurs and a stress of up to 3570 psi results. At the strain rate four times slower, Figure 8B, little work hardening occurs and the stress is decreased by almost an order of magnitude to 500 psi. At the high temperature portion of the of the cycle, and the slower strain rate, the substructure recovers faster than it work hardens which tends to minimize the subsequent recrystallization and growth of the solder microstructure.

The isothermal fatigue tests in this study showed that at room temperature and above heterogeneous coarsening and failure occurs rapidly while at -55°C no coarsening or failure was evident. At -55°C there is simply not enough thermal energy for any coarsening to occur. At room temperature and above the solder joints do fail by a process of heterogeneous coarsening preceding eventual failure. Solomon[16] has shown for isothermal fatigue that a decrease in strain rate results in a decrease in cycles to failure. This observation is contrary to the results here for thermomechanical fatigue which indicates that there is an inherent difference between isothermal and thermomechanical fatigue. This work shows that the response of eutectic Pb-Sn to thermomechanical cycling cannot be predicted from isothermal testing. In addition, the effect of strain rate on thermomechanical fatigue may not be modelled correctly from isothermal tests either. More testing is necessary to establish the mechanistic and quantitative response of eutectic Pb-Sn to thermomechanical cycling.

CONCLUSIONS

Two main conclusions can be made from this work. First the isothermal fatigue response of 60Sn-40Pb solder differs from that of thermomechanical fatigue. In isothermal fatigue a single mechanism dominates during each test (at -55°C it is dislocation processes, and at elevated temperatures it is a diffusive flow mechanism). For thermomechanical fatigue, in the temperature range studied, each cycle the deformation mechanism changes from dislocation processes to diffusional flow. Secondly, variations in strain rate have a large effect of the thermomechanical fatigue behavior. At slower strain rates the dislocation substructure recovers faster than it work hardens which tends to minimize the subsequent recrystallization and heterogeneous growth of the solder microstructure. This result is the opposite of that found for isothermal fatigue. These two conclusions indicate that the response of 60Sn-40Pb solder joints in thermomechanical fatigue can not be predicted using isothermal fatigue testing.

ACKNOLEDGEMENTS

The authors would like to thank J. Finch for invaluable help in performing the isothermal and thermomechanical fatigue tests. This work was supported by the U.S. Department of Energy under contract number DE-AC04-76DP00789.

REFERENCES

1) J. H. Lau, D. W. Rice, "Solder joint fatigue in surface mount technology: state of the art," Solid State Tech., pp. 91-101, Oct. 1985.
2) P. M. Hall, T. D. Dudderar, J. F. Argyle, "Thermal deformations observed in leadless ceramic chip carriers surface mounted to PWBs," IEEE CHMT-6, vol. 6, p.544, 1983.
3) R. N. Wild, "Fatigue properties of solder joints," Welding Research Supp., vol. 51, p. 521s, 1972.
4) E. A. Wright, W. M. Wolverton, "The effect of the solder reflow method and joint design on the thermal fatigue life of leadless chip carrier solder joints," Proc. 34th Electron Components Conf., vol. 34, p. 149, 1984.
5) R. Yenawine, M. Wolverton, A. Burkett, B. Waller, B. Russel, D. Spritz,"Today and tomorrow in soldering," Proc. 11th Naval Weapon Electronics Manufacturing Seminar, China Lake, p. 339, 1987.
6) H. B. Ellis, "Aspects of surface mounted chip carrier solder joint reliability," Proc. 11th Naval Weapon Electronics Manufacturing Seminar, China Lake, p. 377, 1987.
7) D. R. Frear, "Thermomechanical Fatigue of Solder Joints: A New Comprehensive Test Method", Proc. 39th Electron. Comp. Con, vol. 39, p. 293-300, 1989.
8) D. Frear, D. Grivas, M. McCormack, D. Tribula, J. W. Morris, Jr.,"Fatigue and thermal fatigue testing of Pb-Sn solder joints", Proc. 3rd Ann. Electronic Packaging and Corrosion in Microelectronics Conf., vol. 3, p. 269-274, 1987.
9) D. Frear, D. Grivas, J. W. Morris, Jr., "A microstructural study of the thermal fatigue failures of 60Sn-40Pb solder joints", J. Electron. Mats., vol. 17, pp. 171-180.
10) D. Frear, D. Grivas, J. W. Morris, Jr., "Parameters affecting thermal fatigue behavior of 60Sn-40Pb solder joints", J. Electron. Mats., vol. 18, pp. 671-680, 1989.
11) D. Frear, D. Grivas, J. W. Morris, Jr., "Thermal fatigue in solder joints", J. of Metals, vol. 40, pp. 18-22, 1988.
12) C. A. Harper, Handbook of Materials and Process for Electronics, McGraw-Hill, 1971, p. 9-71.
13) A. C. Chilton, M. A. Whitmore, W. B. Hampshire, "Fatigue failure in a model SMD joint", Soldering and Surface Mount Tech., Oct. 1989, no. 3, pp. 21-24, 1989.